Current-Constrained Finite-Time Control Scheme for Speed Regulation of PMSM Systems with Unmatched Disturbances

Huiming Wang, *Member, IEEE,* Zhize Zhang, Yingjie Luo, Junxiao Wang, *Senior Member, IEEE,* Jiankun Sun, *Member, IEEE,* Yunda Yan, *Senior Member, IEEE,* Xianlun Tang, *Senior Member, IEEE*

***Abstract*—The article investigates the speed regulation of permanent magnet synchronous motor (PMSM) systems. Existing control methods of the non-cascade structure suffer from the drawbacks of unsatisfactory anti-disturbance performance and slow convergence rate when the system is affected by disturbances, especially unmatched disturbances. Meanwhile, the requirements of current constraint and fast dynamics cannot be effectively balanced in the single-loop structure of speed and current using traditional control methods such as the PID controller. Because large transient currents induced by fast dynamics may damage the hardware of the system. Therefore, a current-constrained finite-time control approach is proposed. Specifically, a robust finite-time control scheme is developed with the assistance of the improved finite-time observer technique. The proposed method is capable of actively suppressing both matched and unmatched disturbances in non-cascade control systems. Simultaneously, an effective penalty mechanism is established to incorporate a specific gain function into the designed controller. This approach restricts the q-axis current to a predefined safe range without solving an optimization problem. Finally, comparative experiment results indicate that the newly proposed finite-time control method outperforms the baseline control methods in terms of disturbance rejection, convergence rate, and current constraint.**

***Note to Practitioners*—This paper addresses practical challenges in controlling permanent magnet synchronous motor (PMSM) systems, such as ensuring robust disturbance rejection while limiting transient currents to protect the hardware. Traditional methods often fail to balance fast dynamics with current constraints, leading to inefficiencies and potential damage. To tackle these issues, the proposed finite-time control approach introduces a practical solution that achieves robust disturbance rejection while ensuring that transient currents remain within safe operational limits. The use of an improved finite-time observer allows for real-time estimation of system disturbances, while the novel penalty mechanism restricts the q-axis current, preventing hardware damage. This method is particularly suited for applications in robotics, electric vehicles, and automated manufacturing, where precise speed regulation and reliability are crucial.**

***Index Terms*—Current constraint, finite-time control, permanent magnet synchronous motor, unmatched disturbance.**

This work was supported in part by the National Natural Science Foundation of China (62273306, 62373159), in part by the Natural Science Foundation Project of Chongqing, PR China (CSTB2024NSCQ-LZX0026), and in part by the Science and Technology Research Program of Chongqing Municipal Education Commission (KJQN202200626, KJZD-M202200603). (Corresponding author: Huiming Wang).

Huiming Wang, Zhize Zhang, Yingjie Luo and Xianlun Tang are with the Chongqing Key Laboratory of Complex Systems and Autonomous Control, and also with the Key Laboratory of Big Data Intelligent Computing, Chongqing University of Posts and Telecommunications, Chongqing 400065, China (e-mail: wanghm@cqupt.edu.cn; s210301072@stu.cqupt.edu.cn; lyj2258977693@163.com; tangxl@cqupt.edu.cn).

Junxiao Wang is with the College of Information Engineering, Zhejiang University of Technology, Hangzhou 310023, China (e-mail: wjx2017@zjut.edu.cn).

Jiankun Sun is with the School of Artificial Intelligence and Automation, Huazhong University of Science and Technology, and also with the Key Laboratory of Image Processing and Intelligent Control of Education Ministry of China, Wuhan 430074, China (e-mail: sunjiankun@hust.edu.cn).

Yunda Yan is with the Department of Computer Science, University College London, London, WC1E 6BT, UK (e-mail: yunda.yan@ucl.ac.uk).

I. Introduction

In recent years, permanent magnet synchronous motor (PMSM) has aroused tremendous attention due to its fine properties of high torque/power density and torque-to-inertia ratio [1]. As a result, PMSM finds its applications in various fields like aerospace [2], robotics [3], and electric vehicles [4], [5]. In these applications, achieving superior speed regulation performance is of great importance to ensure efficient and reliable operation. Conventionally, the speed regulation of PMSM is achieved through a cascade control structure where the fast inner loop controls the current while the slow outer loop regulates the speed. Recent studies have shown that a non-cascade control structure is more effective and straightforward in regulating the speed when the difference between control periods of the two loops is minimal [6]–[10]. In comparison with cascaded systems, non-cascaded systems are distinguished by a simpler structure and easier-to-adjust parameters. Moreover, non-cascaded systems are less susceptible to the effects of "trial-and-error" parameter tuning methods [11]. In this context, designing an adequate non-cascade control scheme is the focus of this paper.

It is worth noting that the control performance of PMSM systems is normally deteriorated by various disturbances, especially unmatched disturbances [12]. To address the disturbances, many scholars concentrate on observer techniques and observer-based robust control strategies [13]–[19]. Observers are commonly used to construct unmeasured states and disturbances of a system, and then the estimates can be utilized by feed-forward compensations such that proper anti-disturbance performance can be attained. Several elegant observers have been presented in the literature to estimate disturbance, such as extended state observer [20], [21], generalized proportional integral observer [22], and finite-time disturbance observer (FDO) [14], [17], [23]. In particular, the FDO has the advantages of finite-time convergence and insensitivity to pertur-

bations [24]. Although finite-time convergence is guaranteed by the power functions of estimation errors, the FDO cannot provide faster convergence than their linear counterparts when the estimation errors are relatively large.

From the viewpoint of feedback control, it should be pointed out that systems with finite-time stability can achieve a faster convergence rate near the equilibrium point and stronger disturbance rejection ability than systems with asymptotic stability [25]. Hence, finite-time control schemes have been proposed in [25]–[27] and are widely applied in various control systems [28]–[33]. To further consider the disturbances of systems, several observer-based finite-time control approaches have been suggested in [14], [16], [17]. However, the finite-time stability of a system with disturbances may not be guaranteed by these observer-based finite-time controllers. Another shortcoming is that these observer-based approaches, while effective in suppressing disturbances, have difficulty in dealing with overcurrent problems of PMSM systems.

Although PMSM control systems can achieve promising dynamic performance, this capability usually comes at the cost of large transient currents that may pose a risk of damaging the motor or drive. Traditional non-cascade control schemes, such as PID controllers, are not capable of ensuring that the q-axis current is restricted within a safe range [7], [34]. The reason lies in the fact that these methods often limit the transient current by choosing conservative feedback gains, leading to reduced control performance. In the field of modern control, common solutions used to research the current constraint problem are model predictive control [9], [35], [36] and barrier Lyapunov function-based backstepping control [37], [38]. The model predictive control methods build a rational mechanism combining optimization and feedback, where control actions as a suboptimal solution are obtained by solving an optimization problem with the constraints [9], [39]. However, this method has high computational complexity, depends on accurate models, and is sensitive to modeling disturbances. The barrier Lyapunov functions (BLF) , such as tan-type function [37] and log-type function [38], are used to replace the traditional quadratic Lyapunov candidate in each step of the backstepping method, and the constraints are then satisfied step-by-step with the controller design. However, BLF-based methods can be challenging to implement because they require virtual controllers to meet specific feasibility conditions to fulfill predefined constrained regions [40].

Recently, an improved PID controller for PMSM systems has been designed in [6], where the current constraint is solved by constructing a gain function. It inherits from the BLF-based backstepping the idea that establishes a penalty mechanism in control action to steer the current back when it approaches the predefined barrier. This gain function-based method has also been applied in several constrained plants, such as the Buck converters subject to inductor current constraints [41] and inertially stabilized platforms subject to output constraints [42]. It is important to note that the improved PID control proposed in [6] is a passive disturbance suppression method and thereby its control performance may encounter a large degradation when faced with disturbances, especially unmatched disturbances.

According to the above observations, the primary motivation underlying this study is the recognition that the existing non-cascade methods cannot simultaneously cope with the convergence rate, unmatched disturbance rejection, and current constraint of the PMSM systems [6], [7], [14]. In this regard, this paper proposes a robust finite-time control scheme with several novelties. The contributions of our work are set out below:

1) Two modified FDOs (MFDOs) by augmenting linear terms into classical observers [14] are designed to improve the convergence rate in the case of large estimation errors. To the best of the authors' knowledge, it is the first time that the observers with a hybrid structure are designed and evaluated for PMSM systems.
2) Based on MFDOs, leveraging the fast and accurate estimations as a foundation, a robust finite-time controller is developed to provide the systems with a faster convergence rate and enhanced anti-disturbance ability in comparison to asymptotic controllers. It can actively attenuate disturbances, including both unknown external loads, parameter uncertainties and variations.
3) A specific gain function is incorporated into the controller to establish an effective penalty mechanism, which can achieve current constraints without solving the optimal control problem, thereby offering a simple and efficient solution.
4) The theoretical analysis provides a robust foundation for the feasibility and reliability of the proposed method, demonstrating the finite-time stability of the closed-loop system and the efficacy of the current constraint.

The rest of this article is organized as follows: Preliminaries are given in Sec. II. The main results are detailed in Sec. III. Experimental tests are conducted in Sec. IV. A brief conclusion is presented in Sec. V.

Notations: $\lfloor x \rceil^{\alpha} = |x|^{\alpha}\text{sign}(x)$ with $\text{sign}(\cdot)$ the standard sign function, and then $\text{d}\lfloor x \rceil^{\alpha}/\text{d}x = \alpha|x|^{\alpha-1}$; $\mathcal{S}^{(k)}$ denotes k-th time derivative of $\mathcal{S}(t)$. In this article, arguments for functions may be omitted when the context is sufficiently clear.

II. Preliminaries

A. Relevant Lemmas

Consider system

$$\dot{\boldsymbol{x}} = \boldsymbol{h}(\boldsymbol{x}), \boldsymbol{h}(\boldsymbol{0}) = \boldsymbol{0}, \boldsymbol{x}(0) = \boldsymbol{x}_0, \boldsymbol{x} \in R^n, \tag{1}$$

where $\boldsymbol{h}$ is a continuous function.

Definition 1 (Finite-time stability [25]): System (1) is finite-time stable if it is Lyapunov stable and finite-time convergent. The finite-time convergence indicates that there exists a bounded setting time $T(\boldsymbol{x}_0)$ such that for any solution $\boldsymbol{x}(\cdot)$ with initial condition $\boldsymbol{x}_0$, $\lim_{t\to T(\boldsymbol{x}_0)} \boldsymbol{x}(t) = \boldsymbol{0}$ and $\boldsymbol{x}(t) = \boldsymbol{0}$ for $t \geq T(\boldsymbol{x}_0)$.

Definition 2 (Homogeneity [27]): Consider vector field $\boldsymbol{h}(\boldsymbol{x}) = (h_1(\boldsymbol{x}), \cdots, h_n(\boldsymbol{x}))^T$. If for all $\varepsilon > 0$, there exist constants $r_i > 0, i = 1, \cdots, n$, such that $h_i(\varepsilon^{r_1}x_1, \cdots, \varepsilon^{r_n}x_n) = \varepsilon^{k+r_i}h_i(\boldsymbol{x}), \forall \boldsymbol{x} \in R^n$ with $\mathcal{K} > -\min\{r_i, i = 1, \cdots, n\}$, then $\boldsymbol{h}(x)$ is homogeneous of degree $\mathcal{K}$ regarding dilation $(r_1, \cdots, r_n)$.

Lemma 1 [43]: The following system is finite-time stable:

$$\begin{cases} \dot{x}_0 = x_1 - \lambda_n \lfloor x_0 \rceil^{\frac{n}{n+1}} - \sigma_n x_0, \\ \dot{x}_1 = x_2 - \lambda_{n-1} \lfloor x_1 - \dot{x}_0 \rceil^{\frac{n-1}{n}} - \sigma_{n-1}(x_1 - \dot{x}_0), \\ \quad \vdots \\ \dot{x}_{n-1} = x_n - \lambda_1 \lfloor x_{n-1} - \dot{x}_{n-2} \rceil^{\frac{1}{2}} - \sigma_1(x_{n-1} - \dot{x}_{n-2}), \\ \dot{x}_n = -\lambda_0 \text{sign}(x_n - \dot{x}_{n-1}) - \sigma_0(x_n - \dot{x}_{n-1}) - p(t)/L, \end{cases} \tag{2}$$

where $L > 0$, x_i $(i = 0, \cdots, n)$ is the scalar variable; λ_i and σ_i are appropriate constants; $p(t)$ is a perturbation that satisfies $|p(t)| \leq L$.

Lemma 2 [26]: Considering the system

$$\dot{\boldsymbol{x}} = \boldsymbol{h}(\boldsymbol{x}) + \boldsymbol{g}(\boldsymbol{x}), \boldsymbol{h}(\boldsymbol{0}) = \boldsymbol{0}, \boldsymbol{g}(\boldsymbol{0}) = \boldsymbol{0}, \boldsymbol{x} \in R^n, \tag{3}$$

where $\boldsymbol{h}(\boldsymbol{x})$ is homogeneous of degree $\mathcal{K} < 0$ regarding dilation $(r_1, \cdots, r_n)$. Suppose $\boldsymbol{x} = \boldsymbol{0}$ is a asymptotically stable equilibrium of system $\dot{\boldsymbol{x}} = \boldsymbol{h}(\boldsymbol{x})$. Equilibrium $\boldsymbol{x} = \boldsymbol{0}$ of system (3) is a finite-time stable if for all $\varepsilon \neq 0$, $\lim_{\varepsilon \to 0} g_i(\varepsilon^{r_1} x_1, \cdots, \varepsilon^{r_n} x_n)/\varepsilon^{\mathcal{K}+r_i} = 0, i = 1, \cdots, n$.

Lemma 3 [44]: The following cascaded time-varying system

$$\begin{cases} \dot{x}_1 = f_1(t, x_1) + f_{12}(t, x_1, x_2), \\ \dot{x}_2 = f_2(t, x_2), \end{cases} \tag{4}$$

is finite-time stable if 1) Subsystems $\dot{x}_1 = f_1(t, x_1)$ and $\dot{x}_2 = f_2(t, x_2)$ are finite-time stable; 2) For any fixed and bounded x_2, there exists a positive definite and radially unbounded finite-time bounded function $V(t, x_1)$ satisfying $\dot{V}(t, x_1) \leq \Gamma_1 V(t, x_1) + \Gamma_2$, where Γ_1 and Γ_2 are positive constants.

B. Problem Statement

The dynamic model of a surface-mounted PMSM in the $d-q$ reference frame can be expressed as follows [45]:

$$\begin{cases} \dot{i_d} = \dfrac{1}{L}(-Ri_d + n_p L w i_q + u_d), \\ \dot{i_q} = \dfrac{1}{L}(-Ri_q - n_p L w i_d - n_p \phi_f w + u_q), \\ \dot{w} = \dfrac{1}{J}(-Bw + 1.5 n_p \phi_f i_q - T_L), \end{cases} \tag{5}$$

where w is the angular velocity; T_L is the load torque; n_p is the number of pole pairs; B is the viscous frictional coefficient; ϕ_f and J are the rotor flux linkage and inertia, respectively; R and L are the stator resistance and inductance, respectively; i_d, i_q, u_d, and u_q are the stator currents and voltages of the $d-$ and $q-$axes, respectively. Suppose that the controller of i_d loop works well and steers i_d to zero. By lumping both external disturbances and unknown uncertainties [15], system (5) can be obtained as follows:

$$\dot{w} = K_t i_q + \xi_1, \quad \dot{i_q} = \frac{u_q^*}{L_0} + \xi_2, \tag{6}$$

where u_q^* is the controller output; $K_t = 1.5 n_p \phi_f / J$ is the torque constant; L_0 is the nominal value of L; $\xi_1 = -Bw/J - T_L/J$; $\xi_2 = -Ri_q/L - n_p \phi_f w/L + (u_q/L - u_q^*/L_0) - n_p w i_d$. It is noted that ξ_1, the unmatched disturbance of system (6), enters the system via a different channel from control input u_q^*. In addition, ξ_2 is called the matched disturbance [15].

This paper aims to design a control signal u_q^* such that speed w can converge to its reference w_r in finite time, while the q-axis current is constrained to a predefined safe barrier C, i.e., the current satisfies: $|i_q| < C$.

Herein, the following assumptions are listed.

Assumption 1: For system (6): 1) $\xi_1(t)$ and $\xi_2(t)$ are m-th and p-th differentiable, respectively; 2) $\xi_1^{(m)}$ and $\xi_2^{(p)}$ have Lipschitz constants L_1 and L_2, respectively; 3) The unmatched disturbance is bounded by $|\xi_1(t)| < K_t C$.

Remark 1: It is worth noting that the hypotheses regarding disturbances presented in *Assumption 1:* 1)-2) are general and has been previously used in, for example, [14] and [46]. Furthermore, the hypothesis regarding the bound of disturbance $\xi_1(t)$ in *Assumption 1:* 3) is rational since the mismatch disturbance $\xi_1(t)$ affects the q-axis current through a channel that is separate from the control input and may violate the current constraint, it is reasonable to assume that $\xi_1(t)$ is constrained by the S-related range to meet the constraint requirements [7].

III. Main Results

In this section, two MFDOs are first presented to estimate the matched and unmatched disturbances, respectively. Then, a current-constrained finite-time controller is developed.

A. Observer Design

Although the classic FDO developed in [14] can obtain the exact estimations in a finite time, its convergence rate is rather slow in the case of large estimation errors. Inspired by the prior work in [43], we propose two MFDOs to estimate unmatched disturbance ξ_1 and matched disturbance ξ_2, respectively. They are given as follows:

$$\begin{cases} \dot{\hat{w}} = K_t i_q + v_0, \\ \dot{\hat{\xi}}_{1,i-1} = v_i, i = 1, \cdots, m-1, \dot{\hat{\xi}}_{1,m-1} = v_m, \\ v_0 = -\tau_m L_1^{\frac{1}{m+1}} \lfloor \hat{w} - w \rceil^{\frac{m}{m+1}} - \epsilon_m(\hat{w} - w) + \hat{\xi}_{1,0}, \\ v_i = -\tau_{m-i} L_1^{\frac{1}{m+1-i}} \lfloor \hat{\xi}_{1,i-1} - v_{i-1} \rceil^{\frac{m-i}{m+1-i}} \\ \qquad - \epsilon_{m-i}(\hat{\xi}_{1,i-1} - v_{i-1}) + \hat{\xi}_{1,i}, \\ v_m = -\tau_0 L_1 \text{sign}(\hat{\xi}_{1,m-1} - v_{m-1}) - \epsilon_0(\hat{\xi}_{1,m-1} - v_{m-1}), \end{cases} \tag{7}$$

$$\begin{cases} \dot{\hat{i}}_q = \dfrac{u_q^*}{L_0} + \mu_0, \\ \dot{\hat{\xi}}_{2,j-1} = \mu_j, j = 1, \cdots, p-1, \dot{\hat{\xi}}_{2,p-1} = \mu_p, \\ \mu_0 = -\gamma_p L_2^{\frac{1}{p+1}} \lfloor \hat{i}_q - i_q \rceil^{\frac{p}{p+1}} - \varepsilon_p(\hat{i}_q - i_q) + \hat{\xi}_{2,0}, \\ \mu_j = -\gamma_{p-j} L_2^{\frac{1}{p+1-j}} \lfloor \hat{\xi}_{2,j-1} - \mu_{j-1} \rceil^{\frac{p-j}{p+1-j}} \\ \qquad - \varepsilon_{p-j}(\hat{\xi}_{2,j-1} - \mu_{j-1}) + \hat{\xi}_{2,j}, \\ \mu_p = -\gamma_0 L_2 \text{sign}(\hat{\xi}_{2,p-1} - \mu_{p-1}) - \varepsilon_0(\hat{\xi}_{2,p-1} - \mu_{p-1}), \end{cases} \tag{8}$$

where $\hat{w}$, $\hat{\xi}_{1,i-1}$, and $\hat{\xi}_{1,m-1}$ are the estimated values of w, $\xi_1^{(i-1)}$, and $\xi_1^{(m-1)}$, respectively; $\hat{i}_q$, $\hat{\xi}_{2,j-1}$, and $\hat{\xi}_{2,p-1}$ are

the estimated values of i_q, $\xi_2^{(j-1)}$, and $\xi_2^{(p-1)}$, respectively; $\tau_0, \cdots, \tau_m > 0$, $\epsilon_0, \cdots, \epsilon_m$, $\gamma_0, \cdots, \gamma_p > 0$, and $\varepsilon_0, \cdots, \varepsilon_p$ are the coefficients to be selected. Combining (6), (7), and (8), one obtains

$$\begin{cases} \dot{z}_{1,0} = z_{1,1} - \tau_m L_1^{\frac{1}{m+1}} \lfloor z_{1,0} \rceil^{\frac{m}{m+1}} - \epsilon_m z_{1,0}, \\ \dot{z}_{1,i} = z_{1,i+1} - \tau_{m-i} L_1^{\frac{1}{m+1-i}} \lfloor z_{1,i} - \dot{z}_{1,i-1} \rceil^{\frac{m-i}{m+1-i}} \\ \qquad - \epsilon_{m-i}(z_{1,i} - \dot{z}_{1,i-1}), i = 1, \cdots, m-1, \\ \dot{z}_{1,m} = -\tau_0 L_1 \text{sign}(z_{1,m} - \dot{z}_{1,m-1}) \\ \qquad - \epsilon_0(z_{1,m} - \dot{z}_{1,m-1}) - \xi_1^{(m)}, \end{cases} \tag{9}$$

$$\begin{cases} \dot{z}_{2,0} = z_{2,1} - \gamma_{p+1} L_2^{\frac{1}{p+1}} \lfloor z_{2,0} \rceil^{\frac{p}{p+1}} - \varepsilon_{p+1} z_{2,0}, \\ \dot{z}_{2,j} = z_{2,j+1} - \gamma_{p+1-j} L_2^{\frac{1}{p+1-j}} \lfloor z_{2,j} - \dot{z}_{2,j-1} \rceil^{\frac{p-j}{p+1-j}} \\ \qquad - \varepsilon_{p+1-j}(z_{2,j} - \dot{z}_{2,j-1}), j = 1, \cdots, p-1, \\ \dot{z}_{2,p} \in -\gamma_1 L_2 \text{sign}(z_{2,p} - \dot{z}_{2,p-1}) \\ \qquad - \varepsilon_1(z_{2,p} - \dot{z}_{2,p-1}) - \xi_2^{(p)}. \end{cases} \tag{10}$$

where $z_{1,0} = \hat{w} - w$; $z_{1,i} = \hat{\xi}_{1,i-1} - \xi_1^{(i-1)}$; $z_{1,m} = \hat{\xi}_{1,m-1} - \xi_1^{(m-1)}$; $z_{2,0} = \hat{i}_q - i_q$; $z_{2,j} = \hat{\xi}_{2,j-1} - \xi_2^{(j-1)}$; $z_{2,p} = \hat{\xi}_{2,p-1} - \xi_2^{(p-1)}$ are the estimation errors.

Remark 2: It can be seen from (9) and (10) that, these two observers have the hybrid structure combing linear terms and nonlinear terms. In the case of large estimation errors, the linear terms impose the exponential convergence that ensures the errors converge to the neighborhood around zero with high speed. In the case of small estimation errors, the nonlinear terms can make the error converges to zero in finite time. Therefore, this hybrid structure can avoid the slow convergence of the conventional FDOs (when parameters $\epsilon_i, i = 0, \cdots, m$ and $\varepsilon_j, j = 0, \cdots, p$ are all set to zero, MFDOs (7) and (8) become the FDOs) and linear disturbance observers (LDOs) (when parameters $\tau_i, i = 0, \cdots, m$ and $\gamma_j, j = 0, \cdots, p$ are all set to zero, MFDOs (7) and (8) become the LDOs). It should be noted that this is the first time that MFDOs (7) and (8) are designed and evaluated for PMSM systems.

B. Controller Design

With the estimates provided by MFDOs (7) and (8), the velocity tracking error and an auxiliary variable are denoted as $x_1 = w_r - w$ and $x_2 = -K_t i_q - \hat{\xi}_{1,0}$, respectively, where w_r is the reference velocity. By recalling (6), we have

$$\begin{cases} \dot{x}_1 = x_2 + z_{1,1}, \\ \dot{x}_2 = -K_t u_q^*/L_0 - K_t \xi_2 - v_1, \end{cases} \tag{11}$$

Then, a robust finite-time controller is designed as

$$u_q^* = (k_1 \lfloor x_1 \rceil^{\alpha_1} + k_2 \lfloor x_2 \rceil^{\alpha_2} - K_t \hat{\xi}_{2,0} - v_1) L_0/K_t, \tag{12}$$

where $0 < \alpha_1 < 1$, $\alpha_2 = 2\alpha_1/(1+\alpha_1)$; k_1 and k_2 are the controller gains.

To handle the current constraint problem, a gain function method is introduced into controller (12), and then a robust current-constrained finite-time controller is designed as

$$\begin{aligned} u_q^* = &(-K_t \hat{\xi}_{2,0} - v_1 + k_1 \lfloor x_1 \rceil^{\alpha_1} + [k_2 \\ &+ k_3 \mathcal{F}(x_2, \overline{M}, \underline{M})] \lfloor x_2 \rceil^{\alpha_2}) L_0/K_t, \end{aligned} \tag{13}$$

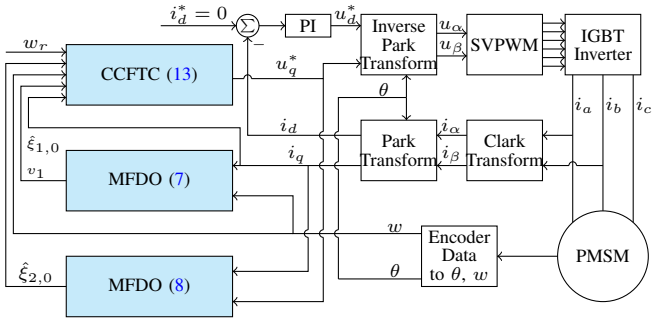

Fig. 1: Block diagram of the suggested PMSM control strategy.

where

$$\mathcal{F}(x_2, \overline{M}, \underline{M}) = \frac{\overline{M}^2}{(\overline{M} - x_2)^2} + \frac{\underline{M}^2}{(\underline{M} - x_2)^2} \tag{14}$$

is the designed gain function with $\underline{M} = -K_t C - \hat{\xi}_{1,0}$, $\overline{M} = K_t C - \hat{\xi}_{1,0}$, and k_3 is the penalty gain. It can be deduced that $-C < i_q(t) < C \Longleftrightarrow \underline{M}(t) < e_2(t) < \overline{M}(t)$.

For simplicity, we denote $k_2^{'} = k_2 + k_3 \mathcal{F}(x_2, \overline{M}, \underline{M})$. By introducing such a gain function, the controller has a large feedback item related to current i_q when it approaches the constraint barrier $\pm C$, resulting in a reactive control action to reduce i_q. The block diagram of the suggested control scheme is illustrated in Fig. 1.

Remark 3: In comparison to existing non-cascade control methods [6], [7], and [14], the novelties of the proposed control method are threefold. First, it incorporates disturbance estimates offered by the constructed MFDOs to actively attenuate not only matched but also unmatched disturbances, enhancing the robustness of the PMSM system. Second, it attains finite-time stability of the closed-loop system by using the designed controller, ensuring a fast convergence rate of the system. Third, it constrains q-axis current in a predefined range by using a specific gain function, improving the hardware safety of the system.

Remark 4: By fusing the MFDO and CCFTC methods, the recommended method addresses three key issues in the speed control system of non-cascaded permanent magnet synchronous motors: limited time convergence, noise suppression and current constraints. The fast and accurate disturbance estimation achieved by the observer enables the constrained finite-time controller to execute robust and safe control actions, which allows the controller to achieve hardware protection without sacrificing dynamic performance. It is worth noting that although one could replace the quadratic term by a higher-order-even power in Equation (14) without affecting the formal proof, such a substitution would make the gain grow even more steeply. In practical applications, the implementation of control signals at discrete time intervals causes the system state to rise more steeply, which in turn causes excessive oscillation of the system state. Hence, quadratic growth strikes a better balance between theoretical rigor and practical robustness.

C. Stability Analysis

Theorem 1: Error systems (9) and (10) are finite-time stable if τ_i, ϵ_i, γ_j, and ε_j, for $i = 0, \cdots, m$ and $j = 0, \cdots, p$, are appropriatly chosen and *Assumption 1* is satisfied.

Proof: Define $y_i = z_{1,i}/L_1$ and $w_j = z_{2,j}/L_2$. Systems (9) and (10) are equivalent to

$$\begin{cases} \dot{y}_0 = y_1 - \tau_m \lfloor y_0 \rceil^{\frac{m}{m+1}} - \epsilon_m y_0, \\ \dot{y}_1 = y_2 - \tau_{m-1} \lfloor y_1 - \dot{y}_0 \rceil^{\frac{m-1}{m}} - \epsilon_{m-1}(y_1 - \dot{y}_0), \\ \quad \vdots \\ \dot{y}_{m-1} = y_m - \tau_1 \lfloor y_{m-1} - \dot{y}_{m-2} \rceil^{\frac{1}{2}} - \epsilon_1(y_{m-1} - \dot{y}_{m-2}), \\ \dot{y}_m = -\tau_0 \text{sign}(y_m - \dot{y}_{m-1}) - \epsilon_0(y_n - \dot{y}_{m-1}) - \dfrac{\xi_1^{(m)}}{L_1}, \end{cases} \tag{15}$$

$$\begin{cases} \dot{w}_0 = w_1 - \gamma_p \lfloor w_0 \rceil^{\frac{p}{p+1}} - \varepsilon_p w_0, \\ \dot{w}_1 = w_2 - \gamma_{p-1} \lfloor w_1 - \dot{w}_0 \rceil^{\frac{p-1}{p}} - \varepsilon_{p-1}(w_1 - \dot{w}_0), \\ \quad \vdots \\ \dot{w}_{p-1} = w_p - \gamma_1 \lfloor w_{p-1} - \dot{w}_{p-2} \rceil^{\frac{1}{2}} - \varepsilon_1(w_{p-1} - \dot{w}_{p-2}), \\ \dot{w}_p = -\gamma_0 \text{sign}(w_p - \dot{w}_{p-1}) - \varepsilon_0(w_p - \dot{w}_{p-1}) - \dfrac{\xi_2^{(p)}}{L_2}. \end{cases} \tag{16}$$

According to *Lemma 1*, systems (15) and (16) are finite-time stable. Then error systems (9) and (10) are finite-time stable based on the definition of y_i and w_j. The proof of *Theorem 1* is thus accomplished.

Theorem 2: The current constraint $|i_q| < C$ holds all the time and the equilibrium of system (11) is finite-time stable, if 1) *Assumption 1* holds, 2) initial state $x_2(0) \in (\underline{M}(0), \overline{M}(0))$, i.e., $i_q(0) \in (-C, C)$, and 3) finite-time controller (13) is employed.

Proof: Three steps make up the procedure: the first two steps prove the finite-time stability of the closed-loop PMSM system, and the last step guarantees the satisfaction of the current constraint.

Step A (Finite-Time Boundedness of System States): Let's start by defining a domain $\Upsilon = \{(x_1, x_2) : x_1 \in (-\infty, +\infty), x_2 \in (\underline{M}(t), \overline{M}(t))\}$. Substituting controller (13) to system (11) yields

$$\dot{x}_1 = x_2 + z_{1,1}, \dot{x}_2 = K_t z_{2,1} - k_1 \lfloor x_1 \rceil^{\alpha_1} - k_2^{'} \lfloor x_2 \rceil^{\alpha_2}. \tag{17}$$

It can be verified from (14) that inequality $0 < k_2^{'} < +\infty$ holds in Υ. Define a finite-time bounded function [44] $V_1(x_1, x_2) = \frac{1}{2}(x_1^2 + x_2^2)$, then

$$\dot{V}_1 = x_1 x_2 + x_1 z_{1,1} - k_1 \lfloor x_1 \rceil^{\alpha_1} x_2 - k_2^{'} |x_2|^{\alpha_2 + 1} + K_t x_2 z_{2,1}. \tag{18}$$

Notice that $|\rho|^{\varphi} < 1 + \varphi|\rho| < 1 + |\rho|$ for $\varphi \in (0, 1)$. With this inequality in mind, it follows

$$\begin{aligned} \dot{V}_1 \leq & |x_1|\,|x_2| + |x_1|\,|z_{1,1}| + k_1 |x_1|^{\alpha_1}\,|x_2| + K_t |x_2||z_{2,1}| \\ \leq & \frac{x_1^2 + x_2^2}{2} + \frac{x_1^2 + z_{1,1}^2}{2} + k_1(1 + |x_1|)|x_2| + K_t \frac{x_2^2 + z_{2,1}^2}{2} \\ \leq & (1 + \frac{k_1}{2})x_1^2 + (\frac{1}{2} + k_1 + \frac{K_t}{2})x_2^2 + (\frac{z_{1,1}^2}{2} + \frac{k_1}{2} + \frac{K_t z_{2,1}^2}{2}) \\ \leq & \Gamma_1 V_1 + \Gamma_2. \end{aligned} \tag{19}$$

where $\Gamma_1 = \max\{2(1 + \frac{k_1}{2}), 2(\frac{1}{2} + k_1 + \frac{K_t}{2})\}$, $\Gamma_2 = \frac{z_{1,1}^2}{2} + \frac{k_1}{2} + \frac{K_t z_{2,1}^2}{2}$. Γ_1 is clearly a bounded constant. According to the finite-time stability of systems (9) and (10), estimation errors $z_{1,1}$ and $z_{2,1}$ converge to zero in a finite time, which indicates that $z_{1,1}$, $z_{2,1}$, and so Γ_2 are bounded. It is deduced based on (19) and the definition of V_1 that system states x_1 and x_2 will not escape to infinity in the finite-time convergent process of the disturbance estimation.

Step B (Finite-time Stability of the closed-loop System): After estimate errors $z_{1,1}$ and $z_{2,1}$ converge to zero in the finite time, system (17) becomes

$$\dot{x_1} = x_2, \quad \dot{x_2} = -k_1 \lfloor x_1 \rceil^{\alpha_1} - k_2^{'} \lfloor x_2 \rceil^{\alpha_2}. \tag{20}$$

A Lyapunov function for system (20) is defined as $V_2 = k_1 \int_0^{x_1} \lfloor s \rceil^{\alpha_1} ds + \frac{1}{2} x_2^2$, and

$$\begin{aligned} \dot{V}_2 = & k_1 \lfloor x_1 \rceil^{\alpha_1} x_2 + x_2(-k_1 \lfloor x_1 \rceil^{\alpha_1} - k_2^{'} \lfloor x_2 \rceil^{\alpha_2}) \\ = & - k_2^{'} |x_2|^{\alpha_2 + 1} \leq 0. \end{aligned} \tag{21}$$

Based on LaSalle's invariant principle, system (20) is asymptotic stable in Υ. Now we denote system (20) as

$$\begin{cases} \dot{\boldsymbol{x}} = \boldsymbol{h}(\boldsymbol{x}) + \boldsymbol{g}(\boldsymbol{x}), \\ \boldsymbol{h}(\boldsymbol{x}) = [h_1(\boldsymbol{x}), h_2(\boldsymbol{x})]^T \\ \qquad = [x_2, -k_1 \lfloor x_1 \rceil^{\alpha_1} - (k_2 + 2k_3) \lfloor x_2 \rceil^{\alpha_2}]^T, \\ \boldsymbol{g}(\boldsymbol{x}) = [g_1(\boldsymbol{x}), g_2(\boldsymbol{x})]^T = [0, [2k_3 - k_3 \mathcal{F}(\cdot)] \lfloor x_2 \rceil^{\alpha_2}]^T, \end{cases} \tag{22}$$

with $\boldsymbol{x} = [x_1, x_2]^T$ is the state vector. It can be concluded according to *Definition 2* that, with respect to the dilation $(r_1, r_2) = (1, (\alpha_1 + 1)/2)$, system $\dot{\boldsymbol{x}} = \boldsymbol{h}(\boldsymbol{x})$ has a homogeneity degree of $\mathcal{K} = (\alpha_1 - 1)/2 < 0$. It is also derived that $\boldsymbol{g}(\boldsymbol{0}) = \boldsymbol{0}$, $\lim_{\varepsilon \to 0} g_1(\varepsilon^{r_1} x_1, \varepsilon^{r_2} x_2)/\varepsilon^{k + r_1} = 0$, and

$$\begin{aligned} \lim_{\varepsilon \to 0} \frac{g_2(\varepsilon^{r_1} x_1, \varepsilon^{r_2} x_2)}{\varepsilon^{k + r_2}} = & \lim_{\varepsilon \to 0} \frac{[2k_3 - k_3 \mathcal{F}(\cdot)] \varepsilon^{\alpha_2 r_2} \lfloor x_2 \rceil^{\alpha_2}}{\varepsilon^{k + r_2}} \\ = & \lfloor x_2 \rceil^{\alpha_2} [2k_3 - k_3 \lim_{\varepsilon \to 0} \mathcal{F}(\varepsilon^{r_2} x_2, \overline{M}, \underline{M})] \\ = & 0. \end{aligned}$$

Based on *Lemma 2*, it can be inferred that system (20) is finite-time stable. Consider the closed-loop system:

$$\begin{cases} System\ (17), \\ System\ (9), \\ System\ (10). \end{cases} \tag{23}$$

With the stability of systems (20), (9), and (10), Lemma 3 leads to the conclusion that closed-loop system (23) is finite-time stable.

Step C (Satisfaction of Current Constraint $|i_q| < C$): Recall the differential equation of x_2:

$$\dot{x}_2(t) = \zeta(x_2,t) = K_t z_{2,1}(t) - k_1 \lfloor x_1(t) \rceil^{\alpha_1} - [k_2 + k_3 \times (\frac{\overline{M}^2(t)}{(\overline{M}(t) - x_2(t))^2} + \frac{\underline{M}^2(t)}{(\underline{M}(t) - x_2(t))^2})] \lfloor x_2(t) \rceil^{\alpha_2} \tag{24}$$

Based on *Definition 1* and the above proof of *Step A* and *Step B*, we know that $x_1(t)$, $x_2(t)$, and $z_{2,1}(t)$ are both bounded in Υ. By considering *Assumption 1*, it can be derived from (24) that for any fixed time $T_1 > 0$,

$$\begin{cases} \lim\limits_{(x_2,t)\to(\overline{M}(T_1),T_1)} \zeta(x_2,t) = -\infty, \\ \lim\limits_{(x_2,t)\to(\underline{M}(T_1),T_1)} \zeta(x_2,t) = +\infty. \end{cases} \tag{25}$$

It can be observed from (25) that there exist a function $\overline{P}(t)$ that satisfies $0 < \overline{P}(t) < \overline{M}(t)$ and a function $\underline{P}(t)$ that satisfies $\underline{M}(t) < \underline{P}(t) < 0$ such that, 1) $\dot{x}_2(t) < 0$ when $x_2(t) \in [\overline{P}(t), \overline{M}(t))$, and 2) $\dot{x}_2(t) > 0$ when $x_2(t) \in (\underline{M}(t), \underline{P}(t)]$. Therefore, dynamic domain $[\underline{P}(t), \overline{P}(t)]$ is an attractor for state x_2. Based on the continuity of solution $x_2(t)$ of system (17) with initial state $x_2(0) \in [\underline{P}(0), \overline{P}(0)] \subseteq (\underline{M}(0), \overline{M}(0))$, it is conclusive that $x_2(t) \in [\underline{P}(t), \overline{P}(t)] \subseteq (\underline{M}(t), \overline{M}(t))$ holds, i.e., current constraint $i_q(t) \in (-C, C)$ holds. ■

In order to summarize the advantages of the proposed method over prior similar methods, the comparisons of the concerned aspects are provided in TABLE I, which indicates that the designed control method has the merit of simultaneously achieving the finite-time stability, attenuation of matched and unmatched disturbances, and current constraint of the system.

IV. Experiment Results

To verify the superiority of the proposed control method, experiments are conducted on a real-time PMSM platform shown in Fig. 2. The motor control experimental platform utilised in this study is based on a TMS320F28335 digital signal processor and a DRV8305 three-phase motor drive. The platform incorporates a pair of Teknic three-phase motors. One motor serves as the controlled PMSM for evaluation of the controller, while the other motor provides the designed load condition during testing. The specification of the investigated PMSM is shown in TABLE II, which can be also referenced in [21]. The following test conditions are used in all the experiments. First of all, the tested controllers are performed using the platform, where the control frequency is set to 10 kHz. In addition, reference speed w_r is set to 1600 rpm, the constraint of q-axis current is 5 A, meaning that $C = 5$ in gain function (14), and the input saturations of u_q and u_d are 12 V. Moreover, for the test of the robustness of the PMSM control systems, load torque T_L is varied from 0 N·m to 0.25 N·m at 2 s in each experiment [47].

A. Efficacy of the proposed method

To validate the proposed current constraint method, we tested four control schemes as follows: MFDO-based current-constrained finite-time control (MFDO+CCFTC) method,

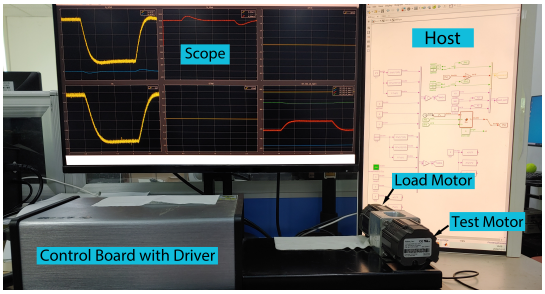

Fig. 2: Experiment platform.

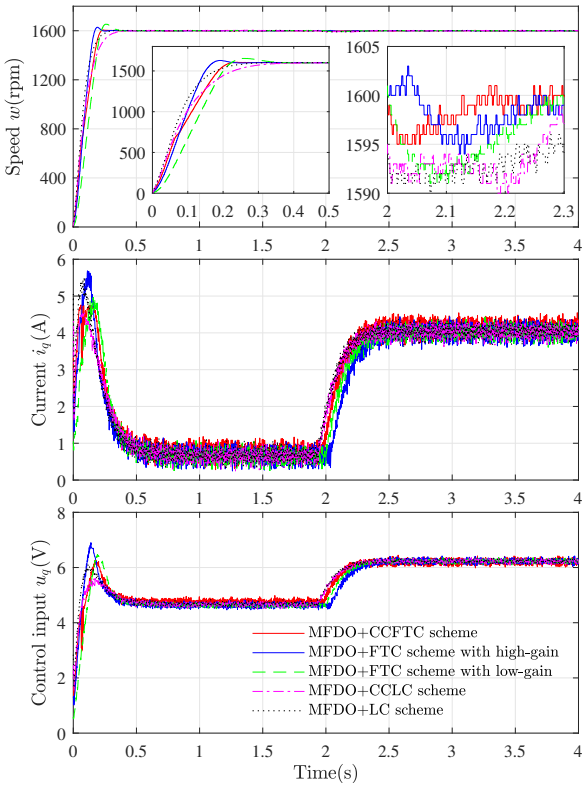

Fig. 3: System responses under MFDO+CCFTC scheme, MFDO+FTC scheme with high-gain, MFDO+FTC scheme with low-gain, MFDO+CCLC scheme, and MFDO+LC scheme: motor speed w, current i_q, and control input u_q^*.

which combines current constraint finite-time controller (13) with gain function $\mathcal{F}(\cdot)$ and MFDOs (7) and (8); MFDO-based finite-time control (MFDO+FTC) method, which combines finite-time controller (12) with MFDOs (7) and (8); MFDO-based current-constrained linear control control (MFDO+CCLC) method, which combines current constraint linear control (when parameters $\alpha_1 = \alpha_2 = 1$ in controller (13) , CCFTC (13) become the CCLC) with gain function $\mathcal{F}(\cdot)$ and MFDOs (7) and (8); MFDO-based linear control (MFDO+LC) method, which combines linear controller with MFDOs (7) and (8). For the MFDO+CCFTC method, the parameters are chosen as: $\{L_1, \tau_0, \tau_1, \tau_2, \epsilon_0, \epsilon_1, \epsilon_2, L_2, \gamma_0, \gamma_1, \varepsilon_0, \varepsilon_1, k_1, k_2, k_3, \alpha_1\} = \{9^5, 1.1, 1.5, 2, 30, 60, 80, 9^5, 1.1, 1.5, 30, 60, 13000, 200, 0.5, 0.6\}$. As for the MFDO+FTC method, two group parameters are selected. In the first group,

TABLE I
Comparisons with prior similar methods

Criterion / Method	Convergence time	Matched and unmatched disturbance rejection	Current constraint
Nonsingular terminal sliding mode control [14]	**Finite-time (Finite-time stability)**	Finite-time disturbance estimation and compensation	✗
Constraint state feedback control [9]	Infinity (Asymptotical stability)	Passive integral action	✓
Current-constrained control [6]	Infinity (Asymptotical stability)	Passive integral action	✓
Disturbance observer-based current-constrained control [7]	Infinity (Asymptotical stability)	Asymptotical disturbance estimation and compensation	✓
The proposed control	**Finite-time (Finite-time stability)**	**Improved finite-time disturbance estimation and compensation**	✓

TABLE II
Key parameters of the investigated PMSM

Parameter	Values	Unit
Rated power	0.426	kW
Rated torque	0.273	N·m
Rated current	7.1	A
Rated speed	1500	rpm
Stator resistance	0.72	Ω
Stator inductance	0.4	mH
Motor inertia	7.06×10^{-4}	kg·m^2
Flux linkage	0.0064	wb
Number of poles	4	–

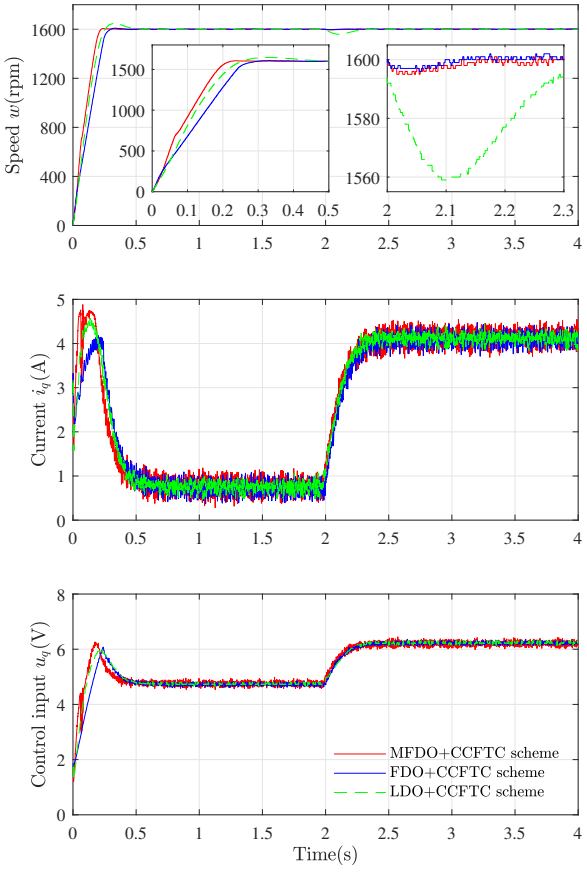

Fig. 4: System responses under MFDO+CCFTC , FDO+CCFTC and LDO+CCFTC schemes: motor speed w, current i_q, and control input u_q^*.

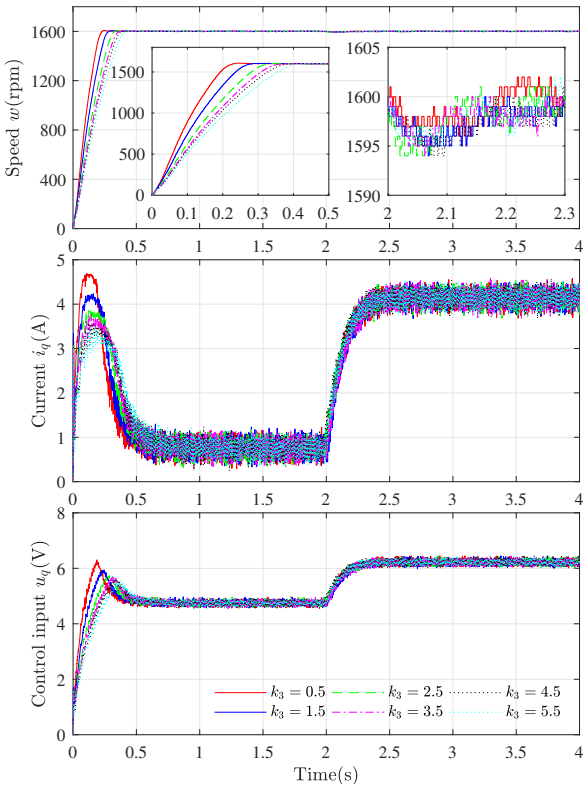

Fig. 5: System responses under MFDO+CCFTC scheme with different k_3: motor speed, current i_q, and control input u_q^*.

controller gain k_1 is set relatively high ($k_1 = 10000$) in order to achieve fast transient performance, while in the other group, controller gain k_1 is set relatively low ($k_1 = 4500$) to meet the current constraint. As for the MFDO+CCLC and MFDO+LC method, controller gain k_1 is set relatively low ($k_1 = 3000$) to meet the current constraint. Other parameters in the two groups are identical to those in the MFDO+CCFTC method.

Fig. 3 displays response profiles of w, i_q, and u_q^* under different controllers. It indicates that both the MFDO+CCFTC and high-gain MFDO+FTC strategies achieve similar transient responses with faster convergence rates than the low-gain MFDO+FTC , MFDO+CCLC and MFDO+LC strategy. The speed overshoots under the MFDO+CCFTC, high-gain MFDO+FTC, and low-gain MFDO+FTC strategies are 8 rpm, 25 rpm, and 13 rpm, respectively. The speed setting times under the MFDO+CCFTC , MFDO+CCLC and MFDO+LC

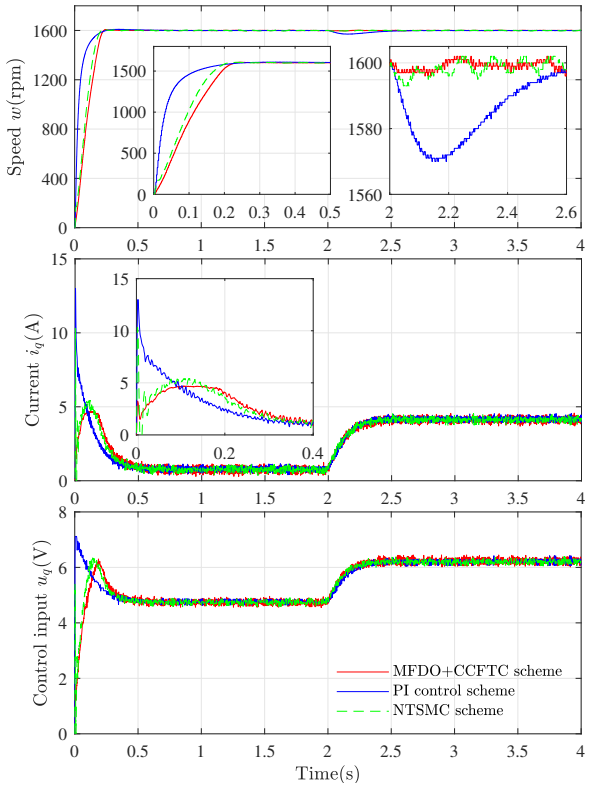

Fig. 6: System responses under MFDO+CCFTC, PI, and NTSMC [14] schemes: motor speed w, current i_q, and control input u_q^*.

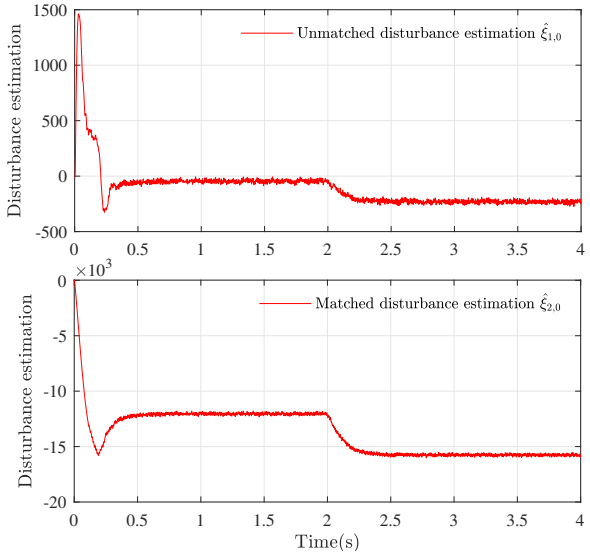

Fig. 7: System responses under the present MFDO+CCFTC scheme: unmatched disturbance estimation $\hat{\xi}_{1,0}$ and matched disturbance estimation $\hat{\xi}_{2,0}$.

strategies are 0.206 s, 0.395 s and 0.310 s, respectively. All four controllers exhibit strong robustness against the sudden load disturbance at 2 s, with a speed drop within 10 rpm. Importantly, the maximum transient current under the MFDO+CCFTC scheme is less than the predefined barrier of 5 A, whereas it fails to achieve this fine property under the high-gain MFDO+FTC scheme and MFDO+LC scheme. Although current i_q under the low-gain MFDO+FTC scheme and MFDO+CCLC scheme also meets this constraint, its dynamic performance and anti-disturbance ability exhibit a large degradation. In summary, the results shown in Fig. 3 demonstrate the efficacy and superiority of the proposed current-constrained method.

To verify the superiority of the proposed MFDOs, we tested three control schemes as follows. The first scheme is the MFDO+CCFTC method mentioned earlier and its parameters are tuned the same as before. The second scheme is the FDO+CCFTC, where the coefficients $\epsilon_0, \epsilon_1, \epsilon_2, \varepsilon_0, \varepsilon_1$ are set to zero in comparison to the MFDO+CCFTC method. The third scheme is the LDO+CCFTC, where the coefficients $\tau_0, \tau_1, \tau_2, \gamma_0, \gamma_1$ are set to zero in comparison to the MFDO+CCFTC and LDO+CCFTC method. Fig. 4 shows response profiles of w, i_q, and u_q^* under these three controllers. It can be seen that the MFDO+CCFTC scheme outperforms the FDO+CCFTC and LDO+CCFTC scheme in terms of dynamic performance, with speed overshoots of 8 rpm, 20 rpm and 47 rpm, respectively. Regarding disturbance rejection performance, MFDO+CCFTC method and FDO+CCFTC method exhibit promising performance, with a speed drop within 6 rpm. However, the speed drop of the LDO+CCFTC scheme reached 41 rpm, thus indicating that the LDO+CCFTC scheme is significantly less effective than the MFDO+CCFTC scheme and FDO+CCFTC scheme in terms of suppressing disturbance. These results suggest that the proposed MFDO+CCFTC method has certain advantages in estimating and suppressing disturbances. As a result, better dynamic performance is also attained by the presented MFDO+CCFTC scheme.

To illustrate the effect of the penalty gain k_3 on the transient current, Fig. 5 gives system responses under MFDO+CCFTC with different values of k_3 while all other parameters remain the same as before. It can be observed that the smaller the k_3, the better the dynamic performance and the higher the maximum transient current, while the current constraint is always maintained. Therefore, both the dynamic performance and the transient current should be considered to adjust k_3.

B. Comparison with existing methods

To further confirm the superiority of the proposed MFDO+CCFTC scheme, we will compare it with the nonsingular terminal sliding mode control (NTSMC) scheme [14] and the PI control scheme. The PI controller is expressed as: $u_q^* = k_p x_1 + k_i \int_0^t x_1(\tau)d\tau$, where k_p and k_i are the controller gains. The NTSM controller is expressed as [14]: $u_q^* = -L_0\hat{\xi}_{2,0} - \frac{L_0}{K_t}(v_1 + \beta_1 \frac{q}{p} x_2^{2-\frac{p}{q}} - K_1 s - K_2 \lfloor s \rceil^\theta)$, where $s = x_1 + \frac{1}{\beta_1} x_2^{\frac{p}{q}}$; the designed constants $\beta_1 > 0$ and $0 < \theta < 1$, positive odd integers p and q, and controller gains K_1 and K_2 are used. To ensure fairness, NTSMC uses the same disturbance estimations as the MFDO+CCFTC scheme, which are provided by MFDOs (7) and (8).

The parameters of the MFDO+CCFTC scheme, in this case, are still as originally given. The proportional gain k_p and integral gain k_i of the PI controller are set to 0.15 and 1.5, respectively. As for the NTSMC scheme, the

parameters are chosen as follows: $\{\beta_1, \theta, p, q, K_1, K_2\} = \{2000, 0.6, 5, 3, 5000, 5000\}$.

The response profiles of w, i_q, and u_q^* under the three controllers (MFDO+CCFTC, NTSMC, and PI control) are depicted in Fig. 6. It is evident from this figure that all three controllers obtain similar dynamic performance. The speed overshoots of the PMSM under MFDO+CCFTC, NTSMC, and PI control methods are 8 rpm, 7 rpm, and 10 rpm, respectively. The curves of the q-axis current reveal that maximum transient currents under the NTSMC and PI control methods exceed the limit of 5 A, registering at 10.33 A and 13.00 A respectively, while the MFDO+CCFTC strategy yields a maximum transient current of 4.69 A, which is well within the constrained range. Regarding the anti-disturbance test, it can be clearly seen that the MFDO+CCFTC and NTSMC strategies both achieve fine performance, while the speed under the PI control strategy suffers a large deterioration. Specifically, the speed drop under the MFDO+CCFTC, NTSMC, and PI control methods are 4 rpm, 7 rpm, and 30 rpm respectively. These results indicate that the proposed MFDO+CCFTC method exhibits superior performance in resisting unmatched load disturbance compared to the NTSMC and PI control methods.

It is noted from system model (6) that, the matched and unmatched disturbance ξ_1 and ξ_2 can occur not only when the load is changed, but also when the PMSM is affected by parameter uncertainties. To show this and verify the effectiveness of the MFDOs in the proposed strategy, the response curves of the unmatched disturbance estimation $\hat{\xi}_{1,0}$ and the matched disturbance estimation $\hat{\xi}_{2,0}$ are presented in Fig. 7. The estimations in this figure are incorporated into controller (13) for disturbance compensation, thereby enhancing the ability of the PMSM system to reject the unmatched and matched disturbances, as also illustrated in Fig. 3-Fig. 6.

The experiment results shown in Fig. 3-Fig. 7 have demonstrated the effectiveness and superiority of the proposed MFDO+CCFTC method. Utilizing these results, related control performance indices of the different schemes, including overshoot (OS), setting time (ST), peak current (PC), and speed drop (SD) under the load variation, are calculated and listed in TABLE III. It can be concluded that the proposed approach delivers promising dynamic performance and anti-disturbance behavior while ensuring that the current is constrained within the predefined range.

TABLE III
Performance indices of the tested schemes

Performance	OS(rpm)	ST(s)	PC(A)	SD(rpm)
MFDO+CCFTC	8	0.206	4.686	4
MFDO+FTC(high gain)	25	0.185	5.792	6
MFDO+FTC(low gain)	13	0.273	4.604	8
MFDO+CCLC	0	0.395	4.551	8
MFDO+LC	2	0.310	5.524	7
FDO+CCFTC	20	0.262	4.246	6
LDO+CCFTC	47	0.475	4.565	41
PI	10	0.166	13.000	30
NTSMC	7	0.188	10.330	7

Remark 5: It's worth noting that the recommended control approach is relatively simple to follow and implement and is also accompanied by a rigorous analysis in Section III.C to guarantee its feasibility. Firstly, the resulting controller (13) follows a common state-feedback form used in finite-time control, which makes it handily understandable. Secondly, unlike many methods requiring optimal control over a finite horizon, our scheme directly incorporates gain function (14) into controller (13), simplifying implementation and reducing the computational effort. Thirdly, observers (7) and (8) can be simplified by properly choosing orders m and p according to the nature of the unmatched and matched disturbances ξ_1 and ξ_2. Therefore, the scheme is compatible with various microprocessors, as demonstrated with the TMS320F28335 DSP at a 10 kHz control frequency in the experiments.

V. Conclusion

In this paper, the current-constrained finite-time control scheme for PMSM systems subject to unmatched and matched disturbances has been investigated via a non-cascade structure. By combining the estimates attained from the MFDOs, the gain function, and the finite-time control, a robust current-constrained finite-time control scheme, which can actively suppress the disturbances and restrict the q-axis current within the preset range, has been designed. In view of the strong robustness against the unmatched disturbance and the satisfaction of the current constraint, this work may be attractive for engineering applications. It should be noted that the recommended control method requires high-performance controller hardware for practical application and can be directly applied to other similar systems, such as induction motors and switch reluctance motors. A promising avenue for future research involves extending the recommended control method to the domain of adaptive control.

References

[1] J. Yang, W.-H. Chen, S. Li, L. Guo, and Y. Yan, "Disturbance/uncertainty estimation and attenuation techniques in PMSM drives—A survey," *IEEE Trans. Ind. Electron.*, vol. 64, no. 4, pp. 3273–3285, Apr. 2017.

[2] H. Li, W. Li, and H. Ren, "Fault-tolerant inverter for high-speed low-inductance BLDC drives in aerospace applications," *IEEE Trans. Power Electron.*, vol. 32, no. 3, pp. 2452–2463, Mar. 2017.

[3] V. M. Hernández-Guzmán and J. Orrante-Sakanassi, "PID control of robot manipulators actuated by BLDC motors," *Int. J. Control*, vol. 94, no. 2, pp. 267–276, 2021.

[4] K.-M. Choo and C.-Y. Won, "Design and analysis of electrical braking torque limit trajectory for regenerative braking in electric vehicles with PMSM drive systems," *IEEE Trans. Power Electron.*, vol. 35, no. 12, pp. 13 308–13 321, Dec. 2020.

[5] K. Rsetam, J. Khawwaf, Y. Zheng, Z. Cao, and Z. Man, "Fast finite-time composite controller for vehicle steer-by-wire systems with communication delays," *World Electric Vehicle Journal*, vol. 15, no. 4, p. 132, 2024.

[6] T. Guo, Z. Sun, X. Wang, S. Li, and K. Zhang, "A simple current-constrained controller for permanent-magnet synchronous motor," *IEEE Trans. Ind. Inform.*, vol. 15, no. 3, pp. 1486–1495, Mar. 2019.

[7] C. Dai, T. Guo, J. Yang, and S. Li, "A disturbance observer-based current-constrained controller for speed regulation of PMSM systems subject to unmatched disturbances," *IEEE Trans. Ind. Electron.*, vol. 68, no. 1, pp. 767–775, Jan. 2021.

[8] Y. Wang, H. Yu, and Y. Liu, "Speed-current single-loop control with overcurrent protection for PMSM based on time-varying nonlinear disturbance observer," *IEEE Trans. Ind. Electron.*, vol. 69, no. 1, pp. 179–189, Jan. 2022.

[9] T. Tarczewski and L. M. Grzesiak, "Constrained state feedback speed control of PMSM based on model predictive approach," *IEEE Trans. Ind. Electron.*, vol. 63, no. 6, pp. 3867–3875, Jun. 2016.

[10] Z. Zhang, X. Liu, J. Yu, and H. Yu, "Time-varying disturbance observer based improved sliding mode single-loop control of pmsm drives with a hybrid reaching law," *IEEE Trans. Energy Convers.*, Dec. 2023.

[11] A. Hace, K. Jezernik, and A. Sabanovic, "Smc with disturbance observer for a linear belt drive," *IEEE Transactions on Industrial Electronics*, vol. 54, no. 6, pp. 3402–3412, 2007.

[12] Y. Yan, J. Yang, Z. Sun, C. Zhang, S. Li, and H. Yu, "Robust speed regulation for PMSM servo system with multiple sources of disturbances via an augmented disturbance observer," *IEEE ASME Trans. Mechatron.*, vol. 23, no. 2, pp. 769–780, Apr. 2018.

[13] S. Ding, Q. Hou, and H. Wang, "Disturbance-observer-based second-order sliding mode controller for speed control of pmsm drives," *IEEE Trans. Energy Convers.*, vol. 38, no. 1, pp. 100–110, Mar. 2023.

[14] J. Yang, S. Li, J. Su, and X. Yu, "Continuous nonsingular terminal sliding mode control for systems with mismatched disturbances," *Automatica*, vol. 49, no. 7, pp. 2287–2291, Jul. 2013.

[15] W.-H. Chen, J. Yang, L. Guo, and S. Li, "Disturbance-observer-based control and related methods—an overview," *IEEE Trans. Ind. Electron.*, vol. 63, no. 2, pp. 1083–1095, Feb. 2016.

[16] S. Li, H. Sun, J. Yang, and X. Yu, "Continuous finite-time output regulation for disturbed systems under mismatching condition," *IEEE Trans. Autom. Control*, vol. 60, no. 1, pp. 277–282, Jan. 2015.

[17] H. Wang, Y. Zhang, Z. Zhao, X. Tang, J. Yang, I. Chen *et al.*, "Finite-time disturbance observer-based trajectory tracking control for flexible-joint robots," *Nonlinear Dyn.*, vol. 106, no. 1, pp. 459–471, Sep. 2021.

[18] A. Rauf, J. Yang, R. Madonski, S. Li, and Z. Wang, "Sliding mode control of converter-fed DC motor with mismatched load torque compensation," in *Proc. 28th IEEE Int. Symp. Ind. Electron.* IEEE, 2019, pp. 653–657.

[19] H. Hou, X. Yu, L. Xu, K. Rsetam, and Z. Cao, "Finite-time continuous terminal sliding mode control of servo motor systems," *IEEE Transactions on Industrial Electronics*, vol. 67, no. 7, pp. 5647–5656, 2019.

[20] M. Hu, W. Hua, Z. Wang, S. Li, P. Wang, and Y. Wang, "Selective periodic disturbance elimination using extended harmonic state observer for smooth speed control in PMSM drives," *IEEE Trans. Power Electron.*, vol. 37, no. 11, pp. 13 288–13 298, Nov. 2022.

[21] Q. Hou and S. Ding, "Finite-time extended state observer-based super-twisting sliding mode controller for PMSM drives with inertia identification," *IEEE Trans. Transp. Electr.*, vol. 8, no. 2, pp. 1918–1929, Jun. 2022.

[22] H. Wang, Y. Pan, S. Li, and H. Yu, "Robust sliding mode control for robots driven by compliant actuators," *IEEE Trans. Control Syst. Technol.*, vol. 27, no. 3, pp. 1259–1266, May 2019.

[23] W. Shen, L. Shao, D. Liu, J. Wang, and C. Ge, "Event-triggered fcs-mpc with sliding mode observer for permanent magnet synchronous motor servo motion systems," *IEEE Trans. Autom. Sci. Eng.*, early access 2024, DOI: 10.1109/TASE.2024.3377639.

[24] A. Levant, "Higher-order sliding modes, differentiation and output-feedback control," *Int. J. Control*, vol. 76, no. 9-10, pp. 924–941, 2003.

[25] S. P. Bhat and D. S. Bernstein, "Finite-time stability of continuous autonomous systems," *SIAM J. Ccontrol Optim.*, vol. 38, no. 3, pp. 751–766, 2000.

[26] Y. Hong, Y. Xu, and J. Huang, "Finite-time control for robot manipulators," *Syst. Control. Lett.*, vol. 46, no. 4, pp. 243–253, Jul. 2002.

[27] S. P. Bhat and D. S. Bernstein, "Geometric homogeneity with applications to finite-time stability," *Math. Control Signals Syst.*, vol. 17, no. 2, pp. 101–127, 2005.

[28] J. Wang, J. Rong, and J. Yang, "Adaptive fixed-time position precision control for magnetic levitation systems," *IEEE Trans. Autom. Sci. Eng.*, vol. 20, no. 1, pp. 458–469, Jan. 2023.

[29] J. Wang, Q. Jiang, and H. Wang, "Generalized disturbance estimation based continuous integral terminal sliding mode control for magnetic levitation systems," *IEEE Trans. Autom. Sci. Eng.*, early access 2024, DOI: 10.1109/TASE.2024.3369905.

[30] K. Rsetam, Z. Cao, and Z. Man, "Design of robust terminal sliding mode control for underactuated flexible joint robot," *IEEE Transactions on Systems, Man, and Cybernetics: Systems*, vol. 52, no. 7, pp. 4272–4285, 2021.

[31] J. Chen, X. Du, L. Lyu, Z. Fei, and X.-M. Sun, "Accurate finite-time motion control of hydraulic actuators with event-triggered input," *IEEE Transactions on Automation Science and Engineering*, 2023.

[32] Y. Gao, Z. Yin, Y. Zhang, Y. Zhang, D. Yuan, and J. Liu, "Surface-mounted permanent magnet synchronous motor servo system speed control using anti-disturbance enhanced finite-time composite control," *IEEE Transactions on Power Electronics*, 2024.

[33] J. Zhao and G.-H. Yang, "Observer-based finite-time fuzzy adaptive resilient control for uncertain nonlinear systems against deception attacks and unknown dead zones," *IEEE Transactions on Automation Science and Engineering*, 2024.

[34] T. Shi, W. Zou, J. Guo, and Z. Xiang, "Adaptive speed regulation for permanent magnet synchronous motor systems with speed and current constraints," *IEEE Transactions on Circuits and Systems II: Express Briefs*, vol. 71, no. 4, pp. 2079–2083, 2023.

[35] Y. Yan, X.-F. Wang, B. J. Marshall, C. Liu, J. Yang, and W.-H. Chen, "Surviving disturbances: A predictive control framework with guaranteed safety," *Automatica*, vol. 158, p. 111238, 2023.

[36] K. Ali, Z. Cao, K. Rsetam, and Z. Man, "Practical adaptive fast terminal sliding mode control for servo motors," in *Actuators*, vol. 12, no. 12. MDPI, 2023, p. 433.

[37] W. Sun, S.-F. Su, Y. Wu, J. Xia, and V.-T. Nguyen, "Adaptive fuzzy control with high-order barrier lyapunov functions for high-order uncertain nonlinear systems with full-state constraints," *IEEE Trans. Cybern.*, vol. 50, no. 8, pp. 3424–3432, Aug. 2020.

[38] Z. Xu, W. Deng, H. Shen, and J. Yao, "Extended-state-observer-based adaptive prescribed performance control for hydraulic systems with full-state constraints," *IEEE ASME Trans. Mechatron.*, vol. 27, no. 6, pp. 5615–5625, Dec. 2022.

[39] F.-J. Zhao, Y.-F. Gao, X.-F. Wang, H.-Y. Gu, and X.-M. Sun, "Robust model predictive control for nonlinear systems with incremental control input constraints," *IEEE Transactions on Automation Science and Engineering*, 2024.

[40] K. Zhao and Y. Song, "Removing the feasibility conditions imposed on tracking control designs for state-constrained strict-feedback systems," *IEEE Trans. Autom. Control*, vol. 64, no. 3, pp. 1265–1272, Mar. 2018.

[41] W. Chen, Z. Ge, Y. Cheng, H. Du, Q. Du, and M. Yu, "Current-constrained finite-time control algorithm for DC-DC Buck converter," *J. Franklin Inst.*, vol. 358, no. 18, pp. 9467–9482, Dec. 2021.

[42] X. Liu, J. Yang, and P. Qiao, "Gain function-based visual tracking control for inertial stabilized platform with output constraints and disturbances," *Electronics*, vol. 11, no. 7, p. 1137, Apr. 2022.

[43] A. Levant, "Non-homogeneous finite-time-convergent differentiator," in *Proc. 48th IEEE Conf. Decision Control*. Shanghai, China, Dec. 2009, pp. 8399–8404.

[44] S. Li and Y.-P. Tian, "Finite-time stability of cascaded time-varying systems," *Int. J. Control*, vol. 80, no. 4, pp. 646–657, 2007.

[45] Q. Hou, S. Ding, and X. Yu, "Composite super-twisting sliding mode control design for pmsm speed regulation problem based on a novel disturbance observer," *IEEE Trans. Energy Convers.*, vol. 36, no. 4, pp. 2591–2599, Dec. 2021.

[46] A. Chalanga, S. Kamal, L. M. Fridman, B. Bandyopadhyay, and J. A. Moreno, "Implementation of super-twisting control: Super-twisting and higher order sliding-mode observer-based approaches," *IEEE Trans. Ind. Electron.*, vol. 63, no. 6, pp. 3677–3685, Jun. 2016.

[47] K. Rsetam, M. Al-Rawi, A. M. Al-Jumaily, and Z. Cao, "Finite time disturbance observer based on air conditioning system control scheme," *Energies*, vol. 16, no. 14, p. 5337, 2023.

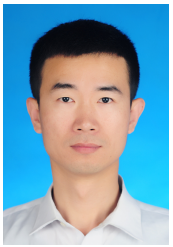

Huiming Wang (Member, IEEE) received the Ph.D. degree from Southeast University, Nanjing, China, in 2016. He was a Research Fellow with the School of Mechanical and Aerospace Engineering, Nanyang Technological University, Singapore, during 2019-2021. He is currently an Associate Professor with the School of Automation, Chongqing University of Posts and Telecommunications, Chongqing, China.

His research interests include the design and applications of advanced control techniques to robotic and mechatronic systems such as high-performance servo drives, industrial robots, and compliant robots.

Zhize Zhang received the B.S. degree in automation from the Guilin University of Electronic Technology, in 2021, and the M.S. degree in control science and engineering from the Chongqing University of Posts and Telecommunications, in 2024.

His research interests include disturbance observer-based control and sliding mode control with application to robotic and mechatronic systems.

Yingjie Luo received the B.S. degree in automation from the Guangdong Ocean University, in 2023. He is currently pursuing the M.S. degree with the Chongqing University of Posts and Telecommunications, Chongqing, China.

His research interests include disturbance observer-based control and position sensorless control of permanent magnet synchronous motors.

Junxiao Wang (Senior Member, IEEE) received the B.S. in automation and the M.S. degrees in control theory and control engineering from School of Information Engineering, Henan University of Science and Technology (HAUST), Luoyang, China in 2008 and 2011, respectively, and the Ph.D. degree in control theory and control engineering from School of Automation, Southeast University (SEU), Nanjing, China, in 2017.

From 2015 to 2016, he was a visiting Ph.D. Student in the Institute for Electrical Drive Systems and Power Electronics, Technical University of Munich (TUM), Munich, Germany. He is currently with the College of Information Engineering, Zhejiang University of Technology, Hangzhou, China. His research interests include generalized disturbance estimation based control and optimization for mechatronic servo drives and autonomous systems.

Dr. Wang was the recipient of 2017 IET Premium Award for best paper in IET Control Theory and Applications (First Author) and the recipient of 2022 Best Paper Award in Control Theory & Applications (First Author). He is an Associate Editor for International Journal of Electronics and Letters.

Jiankun Sun (Member, IEEE) received the B.S. degree in mathematics and applied mathematics from the School of Mathematics from Southeast University, Nanjing, China, in 2013, and the Ph.D. degree in control theory and control engineering from the School of Automation, Southeast University, Nanjing, China, in 2019.He is currently an associate professor with the School of Artificial Intelligence and Automation, Huazhong University of Science and Technology, and also with the Key Laboratory of Image Processing and Intelligent Control of Education, Ministry of China, Huazhong University of Science and Technology.

His current research interests include disturbance/uncertainty estimation and attenuation, learning-based control, active inference, safety-critical control, and unmanned autonomous system.

Yunda Yan (Senior Member, IEEE) received his B.Eng. degree in Automation and Ph.D. in Control Theory and Control Engineering from the School of Automation, Southeast University, Nanjing, China, in 2013 and 2019, respectively. From 2016 to 2023, he held visiting and academic positions at the National University of Singapore, Singapore; Loughborough University, U.K.; and De Montfort University, U.K. In September 2023, he joined the Department of Computer Science at University College London (UCL), U.K., as a Lecturer in Robotics and AI. He is a Senior Member of the IEEE and a Fellow of the Higher Education Academy.

His current research interest focuses on the safety-guaranteed control design for robotics, especially related to optimisation, data-driven and learning-based methods.

Xianlun Tang (Senior Member, IEEE) received the M.S. and Ph.D. degrees from Chongqing University, Chongqing, China, in 2002 and 2007, respectively. He is currently a Professor at the Chongqing University of Posts and Telecommunications.

His current research interests cover pattern recognition and artificial intelligence, computer vision and its applications, and human-computer interaction systems.